ACS APPLIED MATERIALS & INTERFACES

Research Article

www.acsami.org

Electropolymerized Conjugated Polyelectrolytes with Tunable Work Function and Hydrophobicity as an Anode Buffer in Organic Optoelectronics

Sebastian Lacher,[†] Naoki Obata,[†,‡] Shyh-Chyang Luo,[§] Yutaka Matsuo,[†,*] Bo Zhu,[§] Hsiao-hua Yu,[§] and Eiichi Nakamura[†,*]

[†]Department of Chemistry, The University of Tokyo, Hongo, Bunkyo-ku, Tokyo 113-0033, Japan

[‡]Mitsubishi Chemical Group Science and Technology Research Center, Inc., 1000 Kamoshida-cho, Aoba-ku, Yokohama-shi, Kanagawa 227-8502, Japan

[§]Yu Initiative Research Unit, RIKEN Advanced Science Institute, 2-1 Hirosawa, Wako, Saitama 351-0198, Japan

Supporting Information

ABSTRACT: A new class of conductive polyelectrolyte films with tunable work function and hydrophobicity has been developed for the anode buffer layer in organic electronic devices. The work function of these films featuring a copolymer of ethylenedioxythiophene (EDOT), and its functionalized analogues were found to be easily tunable over a range of almost 1 eV and reach values as high as those of PEDOT:PSS. The new buffer material does not need the addition of any insulating or acidic material that might limit the film conductivity or device lifetime. Organic photovoltaic devices built with these films showed improved open-circuit voltage over those of the known PSS-free conductive EDOT-based polymers with values as high as that obtained for PEDOT:PSS. Furthermore, the surface hydrophobicity of these new copolymer films was found to be sensitive to the chemical groups attached to the polymer backbone, offering an attractive method for surface energy tuning.

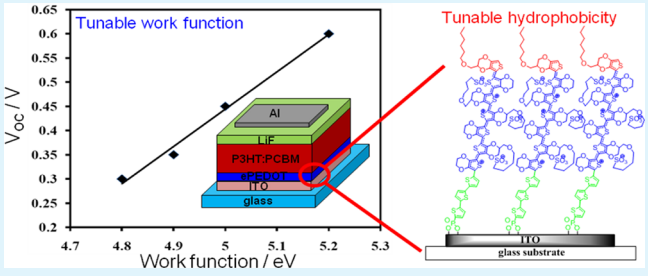

KEYWORDS: *hole-injection layer, work function, surface energy, conductive polymer, organic solar cell*

INTRODUCTION

The efficiencies and lifetimes of organic electronic devices have increased significantly in recent years. New classes of organic semiconductors in the active layer resulted in efficiencies of organic photovoltaics (OPVs) of up to 10%.[1,2] These semiconductors are usually optimized with respect to their energy levels and miscibility to reach the highest possible efficiencies. Despite the well-known fact that the charge injection/extraction layers greatly affect the efficiency and lifetime of such devices,[3−8] optimization of the anode buffer layer for both the work function and the surface energy has often been neglected. Few alternatives to the widely used poly(3,4-ethylenedioxythiophene):poly(*p*-styrenesulfonate) (PEDOT:PSS)[9,10] have been successfully implemented so far, and they usually suffer from high production costs or difficult processing conditions.[11−13] PEDOT:PSS is still the material of first choice because of its high work function and easy processability. Alternative buffer layers, however, are desired, as PEDOT:PSS shows detrimental effects on device lifetime[14] because of its high acidity and etching of ITO.[15−17] In addition, the presence of a large amount of insulating PSS reduces the conductivity of the film, especially in the surface region,[18,19] and leads to hydrophilic films that are often not ideal for the deposition of hydrophobic organic semiconductors.[20] The high concentration of PSS in the surface region, however, is necessary to achieve the high work functions needed for applications.[21,22] Alternative organic films with high work functions usually require the addition of insulating material such as fluorinated sulfonic acid polymer,[23,24] perfluorinated ionomers,[25] or EDOT polymerization with organic semiconductors disturbing the PEDOT conjugation.[26]

In turn, the conductivities of PEDOT films without insulating additives are known to be several orders of magnitude higher than that of commonly used PEDOT:PSS,[27] resulting in increased short-circuit current (J_{SC}) in OPVs.[28−32] However, the application of these highly conductive films in organic electronic devices is limited by their low work function, which leads to charge injection barriers, thereby reducing the device performance. Thus, it is currently necessary to compromise between conductivity and high work function.[33]

We present here a solution to this problem through the development of a new conductive polyelectrolyte with tunable

Received: February 29, 2012
Accepted: June 27, 2012
Published: June 27, 2012

work function that reaches the level commonly observed for PEDOT:PSS but without the need for any acidic or insulating additives such as PSS. Furthermore, we achieved a tuning of film hydrophobicity obtaining films with significantly increased water contact angles. In this proof-of-principle study, we used patterned ITO substrates for building bulk heterojunction OPV devices using poly-3(hexylthiophene) (P3HT) and phenyl-C61-butyric acid methyl ester (PCBM) in the active layer. We studied the relationship between the work function of the anode buffer layer and the V_{OC} of the bulk heterojunction OPV device and found improved V_{OC} values over those of a similar PEDOT-based PSS-free conductive anode buffer.

RESULTS AND DISCUSSION

The anode buffer layer in OPVs greatly affects the device performance, as demonstrated previously by increased conductivity to achieve higher J_{SC} values,[28,34] the establishment of an ohmic contact to increase the V_{OC} value,[35] and the change in the surface energy to control the morphology of the active layer.[36] The exact influence on the work function by the anodic buffer layer is still under debate,[37,38] but recent studies indicate the effective lowering of the charge injection barriers to increase the V_{OC} values in bulk heterojunction OPVs and an increase in the fill factor (FF) in flat heterojunction devices.[39] Clearly, optimization of all of these parameters is necessary to achieve high efficiencies. EDOT-based polymers are well established and known for their stability, conductivity, and transparency.[40,41] Electropolymerized PEDOT (ePEDOT) anode buffers showed improvements in J_{SC} and device lifetime of OPVs compared with PEDOT:PSS because of the replacement of the insulating and acidic PSS with electrochemical dopants such as perchlorate,[29,31,32] leading to highly conductive polymer films.[27] However, the work function of these films has been much less studied and, in fact, the V_{OC} values of these ePEDOT-based OPV devices were found to be low, indicating the presence of a charge injection barrier.

Polymers based on EDOT with covalently bound sulfonate groups (EDOT−SuNa; see Chart 1 for the structures of the compounds used throughout this study) are known for their high conductivity (polymer of EDOT−SuNa shown in Chart 2).[42] Nevertheless, the preparation and processing of this polymer are challenging because it tends to form only water-soluble oligomers.[43] Furthermore, the random distribution of the negative counterions leads to a cancellation of the dipole and hence to the low work function of 4.4 eV.[23,44] We envisioned controlling this distribution of negative counterions by the copolymerization of EDOT with EDOT−SuNa (see Chart 2). This copolymerization strategy has several advantages: (i) the polymers are more hydrophobic, which makes film formation from aqueous solution possible; (ii) the variation of the copolymer ratio allows easy control of the distribution of the counteranions along the polymer backbone; and (iii) the use of monomers with a variety of functional groups, as shown in Chart 1, can influence the surface energy of the films.

Chart 1. EDOT Monomers Used for Electropolymerization and Thiophene-Based Molecules for SAM Formation on ITO

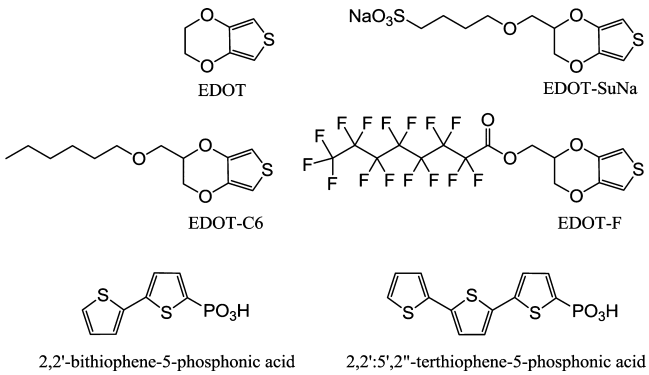

Electropolymerization Procedure. We prepared the polyelectrolyte films starting from ITO modified with self-assembled monolayers (SAMs) as shown in Scheme 1 (step A). Such a surface-initiated polymerization allows us to obtain a better controlled film morphology (i.e., lower surface roughness),[45,46] better film adhesion, and improved electrical contact.[47] It is important to note that the PEDOT film grows only on the ITO part of the substrate, not the glass surface (illustrated in Scheme 1). This produces a different substrate architecture for OPVs compared to that of PEDOT:PSS spin coated substrates that bears the buffer uniformly on the surface (vide infra).

We obtained stable polyelectrolyte films by applying a positive potential to ITO modified with SAMs of 2,2′:5′,2″-terthiophene-5-phosphonic acid and 2,2′-bithiophene-5-phosphonic acid when placed in an EDOT monomer solution (Scheme 1, step B). The films were stable against peeling with Scotch tape, sonication, and electrochemical redox cycles, which is a sign of covalent bond formation between the SAM and the polymer.[48] Covalent bond formation is possible in this case because the oxidation potential of the two molecules is below that of EDOT−SuNa (see Supporting Information, Table S1). On the other hand, the films polymerized on ITO functionalized with 2-thiophene phosphonic acid or triethoxy-2-thienylsilane peeled off under electrochemical cycling, because the oxidation potential of the thiophene SAM was too high to produce thiophene cationic species that could react with EDOT monomers to start the polymerization process. Thus, we suspect that the previously reported improvement of ePEDOT film formation using thiophene SAMs on ITO is not because of covalent bond formation but better film adhesion[28] (see the Supporting Information for the details of the SAM-initiated electropolymerization process).

Note that the covalent linkage of films to ITO made it impossible to determine the film conductivity by the four-point probe technique, while the excellent conductivity data of ePEDOT-based films have been reported previously in numerous reports[18,49−51] with conductivities of 400−450 $S \cdot cm^{-1}$ for tosylate-doped ePEDOT.[27]

The film polymerization was performed from an aqueous solution of 0.01 M EDOT−monomer mixture (EDOT/EDOT−SuNa) containing 0.1 M $LiClO_4$ as electrolyte and 0.01 M sodium dodecylsulfate (SDS), the presence of which significantly reduced the roughness of the film surface.[52−54] The aqueous polymerization system we used in this study has an advantage over polymerization from organic solvents, which often leads to increased surface roughness.[55]

The solution was acidified by HCl to a pH of 2. As a counter electrode, a 25 × 25 mm^2 Pt metal mesh was placed 5 mm from the ITO working electrode. Ag/AgCl was used as a reference electrode. We applied a constant current over a period of 45−90 s to keep the voltage low, which is important for obtaining

Chart 2. Polymer Based on (A) EDOT−SuNa and (B) Copolymer of EDOT/EDOT−SuNa[a]

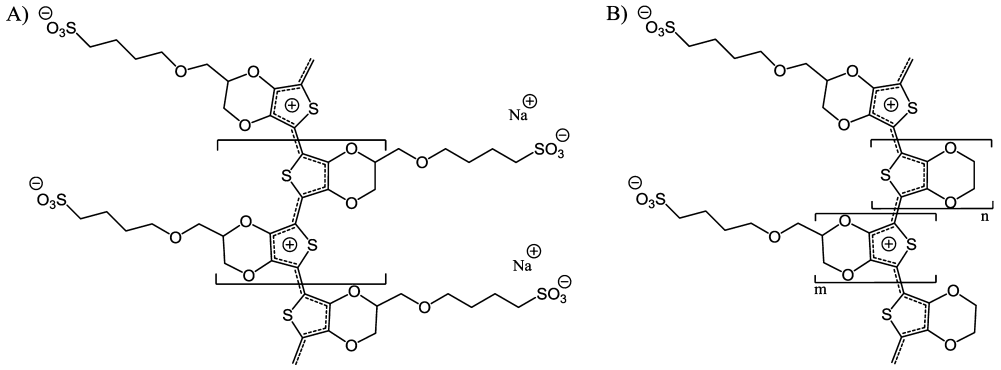

[a]The counterions of the polymer in (A) are equally distributed along the polymer backbone, while those in (B) are dependent on the alignment of EDOT monomers in the copolymer chain.

Scheme 1. Three Steps of Polyelectrolyte Film Formation[a]

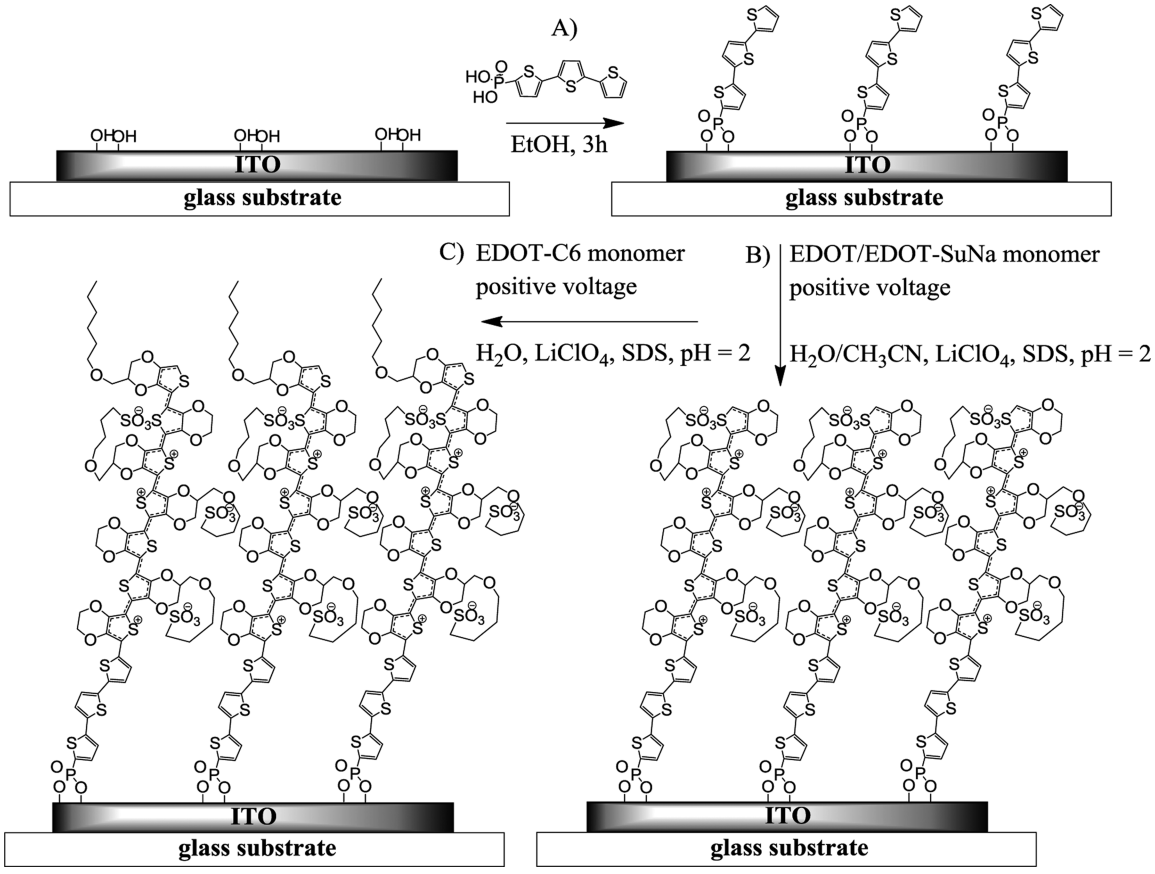

[a](A) Terthiophene phosphonic acids are used to functionalize ITO. (B) The SAM-modified substrate is placed in a solution containing EDOT/EDOT−SuNa monomers. The polymerization occurs only on ITO and is achieved by applying a positive voltage. (C) A short second polymerization step in another solution containing EDOT monomers with a different side chain yields ultrathin top layers.

smooth films.[51] The film thickness was controlled by the applied charge density, which we calibrated as shown in Figure 1. The thickness−current density relationship was the same regardless of the EDOT/EDOT−SuNa ratio, which was controlled by the relative concentrations of the monomers in the solution. The monomer ratio in the electropolymerization solution roughly reflects the ratio in the copolymer.[56] The resulting films were insoluble up to an EDOT−SuNa content of 25%. To obtain polymers with higher EDOT−SuNa content, 20% acetonitrile was added to the polymerization mixture, which allowed us to obtain copolymers with at least 50% EDOT−SuNa without affecting the surface roughness. At EDOT-SuNa concentrations higher than 50% the films became increasingly soluble despite the 20% acetonitrile making it difficult to prepare stable films in aqueous solutions.

After polymerization, the films were rinsed with a large amount of Millipore water (we used such water throughout the study). We followed the procedures reported in ref 50 to remove all ions present in solution that could affect the doping level or conductivity. For that purpose, we washed the film

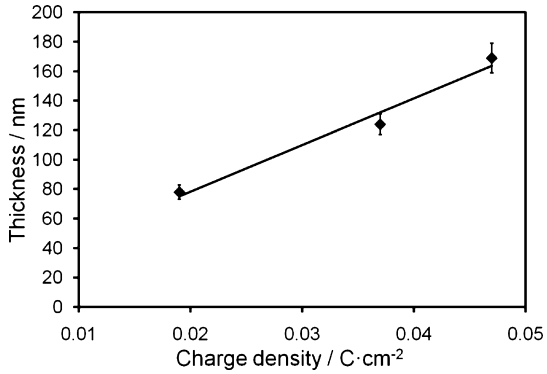

Figure 1. Relationship between the charge density and the film thickness for EDOT/EDOT−SuNa polymer (EDOT−SuNa content: 25%) films polymerized from water. Thickness was determined by AFM.

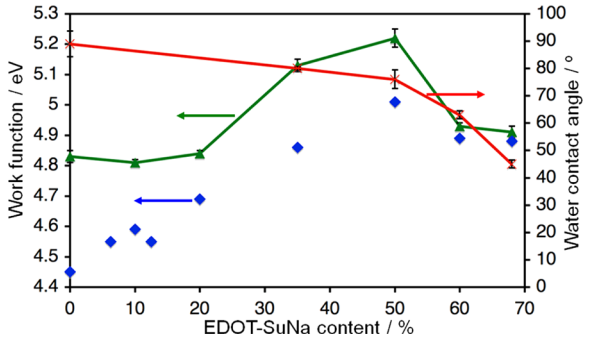

Figure 2. Dependence of the work function and the water contact angle (red line) of EDOT/EDOT−SuNa copolymer films on the EDOT−SuNa content. Work functions of self-doped films are shown as blue diamonds and perchlorate-doped films as green triangles. Exact values are given in Table S2 (Supporting Information).

twice, applying negative voltages to remove anions such as perchlorate and SDS and reduced the film. The first time we used −0.6 V for 300 s in a 0.1 M $LiClO_4$ solution and rinsed the film with water. Then we applied another −0.6 V for 150 s in water to remove the remaining anions in the film. Subsequently, film doping was performed at 0.6 V for 150 s in water (we call the doping process in water "self-doped"). In this case, the attached sulfonate ions take the part of the dopant, leading to self-doped films with high transparency and conductivity (vide infra). Alternatively, we doped the films at 0.6 V for 150 s in 0.1 M $LiClO_4$ (we call these films "perchlorate-doped"). This doping process led to the incorporation of perchlorate ions, which besides the sulfonate ions present can take the part of the dopant.

The charge flow upon doping depends on the film thickness and the EDOT−SuNa content in the film, confirming that the sulfonate groups of the copolymer act as the major source of dopant ions (Supporting Information, Figure S1). Furthermore, the charge flow upon de- and redoping shows a logarithmic behavior, which is consistent with the electrochemically stimulated conformational relaxation (ESCR) model[57] that explains the slow doping process of conductive films with a conformational change of the polymer upon ion diffusion. This doping is faster for polymer layers facing the solution interface, because the pores from the de-doping procedure are still present, often referred to as "memory effect".[58]

The oxidized films were stable under ambient conditions. The work function was measured in vacuum by photoelectron yield spectroscopy (PYS), a method that has proven useful for rapid and reliable determination of work functions.[59]

Film Properties: Work Function. We found a linear relationship between the EDOT−SuNa content and the polyelectrolyte film work function up to 50% EDOT−SuNa for the self-doped films (blue diamonds in Figure 2). The increase in work function for the low EDOT−SuNa content can be explained by the different oxidation levels of the film. Interestingly, at EDOT−SuNa content > 50%, the work function decreases, suggesting that factors other than the film oxidation levels need to be considered. In addition, we observed a similar rise in the work function for the perchlorate-doped films (green triangles in Figure 2) at 50% EDOT−SuNa content in the copolymer.

Note that the self-doped films show much lower work functions at 0−10% EDOT−SuNa content compared with the perchlorate-doped analogues. This was expected, considering the reduced amount of possible counteranions that act as dopants, thereby reducing film oxidation. These results suggest that no other anions act as dopants, and thus all ions were successfully washed out of the films during the washing procedure at negative applied voltage, leaving no insulating material such as SDS in the film.

A possible explanation for the film work function dependence on EDOT−SuNa content is the dipole effect rising from the location of positive and negative charges in the film. The molecular dipole is defined as the product of the value of the partial charge and the distance between the two charges.[59] It has been known for some time that the location of the counterions is crucial for the work function of charged films.[60] In our case, the positive charges are delocalized over the PEDOT π-system, whereas the negative ions are localized on the side of the PEDOT backbone (see Chart 2). The counterions will be fixed on one side of the polymer because of the rigidity of the polymer backbone. A nonrandom distribution of counterions along the polymer backbone will lead to an overall dipole of the polymer chains, which influences the film work function and could explain the observed work function behavior. We envision that the counterion distribution along the polymer backbone is dependent on the EDOT−Na content in the copolymer film and that the highest probability of a nonrandom distribution of sulfonate ions is at an EDOT−SuNa content of 50%. Higher concentrations of EDOT−SuNa will lead to cancellation of dipoles and lower work functions. Finally, with a complete EDOT−SuNa film, the dipoles will completely cancel out (Chart 2), leading to the above-mentioned low work function of 4.4 eV.

Work function tuning with polyelectrolyte buffers has been known for some time;[61] however, its application has been limited to positive ions attached to the polymer backbone to enhance electron injection.[62−69] These polymers are designed in a way that the positive ions are fixed on a specific side of a monomer, forming a semiconducting polymer with the counterions being delocalized in the film. Interfacial dipoles with one pole pointing toward the polymer layer and the other one toward the metal were proposed as a possible way of how these polymers alter the metal work function.[61,70] However, an in-depth discussion of the mechanism has been missing because the net alignment of dipoles at the metal/organic interface and in the bulk polymer is still not understood. Our results here indicate that the arrangement of ions in the bulk film is crucial

for the film work function and can be controlled by the polymer design. Thus, more detailed studies will be necessary to exploit the full potential of polyelectrolyte films.

The higher work function of perchlorate doped films than that of their self-doped counterparts can be explained by the distribution of perchlorate ion location in the film[60] arising from the re-doping process following the above-mentioned ESCR model.[57]

Earlier reports found a high influence of the doping voltage on the work function of conducting polymers.[71−76] When doping the copolymer films at voltages between 0.4 and 0.8 V in water, we could not observe any difference in the work function because the oxidation level is mainly determined by the EDOT−SuNa ratio. After doping these films in 0.1 M $LiClO_4$ solution at different voltages, we measured a small increase in work function of approximately 0.1 eV between the films doped at 0.4 and 0.8 V. This increase is low, and we expect that such a procedure is not suitable for obtaining stably high work function values because of overoxidation effects and the instability of highly oxidized films under ambient conditions. Similar films reported earlier were doped under an inert gas atmosphere and the work function measurement was performed under argon gas.[71] In turn, the work functions of the films reported here were stable under ambient conditions for at least several weeks.

Film Properties: Hydrophobicity. The ability to control the surface properties is a feature of the present copolymerization strategy, as demonstrated through measurements of the contact angles for the ITO covered with a copolymer of a variety of EDOT derivatives and EDOT/EDOT−SuNa. For instance, as studied for the EDOT/EDOT−SuNa copolymer of various EDOT−SuNa contents (Figure 2), the use of more EDOT−SuNa decreased the water contact angle of the copolymer surface, making it more hydrophilic than ePEDOT without EDOT−SuNa by a reduction of the water contact angle from 89° to 45° for an EDOT−SuNa content of 68%. PEDOT:PSS shows a water contact angle 10−12°[77] and absorbs water quickly, which makes a determination of the water contact angle challenging. We did not observe such a behavior for any of the films in Figure 2.

Importantly, we were able to tune the work function and water contact angle independently by introducing different EDOT−SuNa contents in the bulk and in the uppermost film layer. We achieved this by injecting an EDOT−SuNa solution into the polymerization mixture during the polymerization process under stirring of the polymerization solution, which changed the EDOT−SuNa content of the uppermost part of the polymer. The work function of these films was dependent on the overall EDOT−SuNa content in the bulk following the trend in Figure 2, but the hydrophobicity was dependent on the EDOT−SuNa content of the uppermost layer, which was determined by the final EDOT−SuNa content in the polymerization mixture. This procedure is especially appealing because it uses only two monomers and one polymerization step. It is important to note that this procedure did not lead to an increase in surface roughness (see Supporting Information, Figure S5). Using this method, we achieved various contact angles of polymer films below 89°, which is the value that we determined for pure EDOT-based films (Figure 2).

In an attempt to increase the film hydrophobicity, we used different functionalized EDOT monomers bearing hydrophobic hexyl and perfluoroheptyl chains (EDOT-C6 and EDOT-F in Chart 1) to be polymerized on top of the EDOT/EDOT−SuNa films. Such ultrathin top layers were achieved by applying a second polymerization step in a monomer solution of EDOT-C6 and EDOT-F, respectively (see step C in Scheme 1). For the very hydrophobic EDOT-F we used an ionic liquid as the polymerization solvent, which is described in the Supporting Information. To this end, we polymerized a 5 nm thick film of EDOT-C6 and EDOT-F, respectively, which led to an increase in the water contact angle of 15−20°. Interestingly, the presence of these thin top films also increased the film work function by 0.26 eV for films functionalized with EDOT-F and decreased it by 0.04 eV in the case of EDOT-C6 top films. This is consistent with earlier findings of perfluoro side chains on the boundary of organic films influencing the film energy levels.[78]

The results here demonstrate the possibility of work function and surface energy tuning by the side chain of the EDOT monomers. This makes available a large variety of possible combinations of work functions and surface energies through copolymerization of different EDOT monomers. EDOT-F is especially interesting for such applications because of the hydrophobicity of its films[79] and its high conductivities of up to 65 S cm^{-1}.[80] We envision that the good resistance against water penetration and stable work functions should make these films interesting for other possible applications, such as for biological sensors.[81−83]

We could not apply the films covered with the EDOT-C6 or EDOT-F top layer to OPV devices because their very high hydrophobicity made it difficult to spin coat a P3HT:PCBM blend on patterned glass/ITO/ePEDOT substrates, causing active layer fracture (Supporting Information, Figure S8). Therefore, we describe below only the application of EDOT/EDOT−SuNa copolymer for the influence of the work function on V_{OC} of polymer bulk-heterojunction OPV devices.

Film Properties: Surface Roughness and Transparency. The surface roughness of the electropolymerized films was small and in the range of Z_{rms} = 3−4 nm for films of 25−50 nm thickness, as determined by atomic force microscopy (AFM, Figure 3). The roughness increased slightly to Z_{rms} = 5 nm for thicker films of 100 nm (Supporting Information, Figure S2). A low surface roughness is important to prevent the formation of pinholes in OPV devices that can reduce the V_{OC}.[29]

As expected, the transparency of the polyelectrolyte films was enhanced in the visible region after the applied doping procedure and was the same for self-doped and perchlorate-doped films (Figure 4, blue and green lines, respectively).

OPV Devices with Polyelectrolyte Films. Devices with the architecture ITO/buffer/P3HT:PCBM/LiF/Al were built using a 50 nm thick anode buffer layer prepared with different EDOT−SuNa contents either perchlorate-doped (entries 1 and 4, Table 1) or self-doped (entries 2 and 3, Table 1) to investigate the effects of the work function on OPV performance (for the exact device building procedure, see the Supporting Information).

As ITO substrates we used patterned ITO on glass, which are commonly used in the OPV research. Electropolymerizing PEDOT on this substrate led to coverage of only the ITO area (edge issue). In turn, PEDOT:PSS was spin coated over the whole glass slide. We found that the active layer and therefore J_{SC} and FF were influenced by this difference of substrates architecture and by the large difference in hydrophobicity between the glass substrate and the ePEDOT film (wettability issue, both described in the Supporting Information). Due to this influence of the substrate on the active layer, we found it

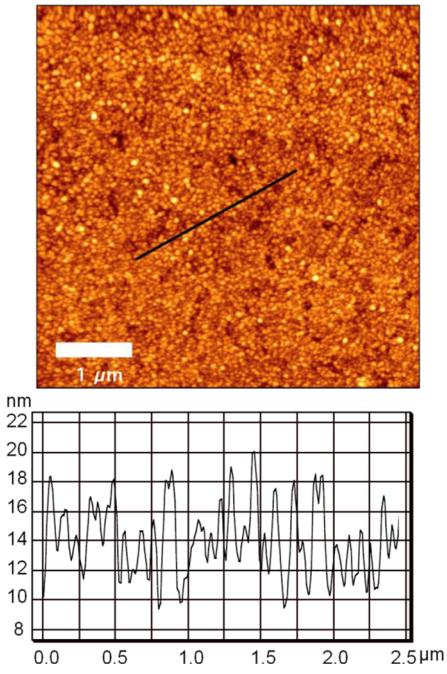

Figure 3. Left: AFM image of a 25 nm polyelectrolyte film with 35% EDOT−SuNa polymerized from water with 20% acetonitrile as cosolvent with a Z_{rms} of 3.2 nm. Right: Height profile of the line shown in the AFM image.

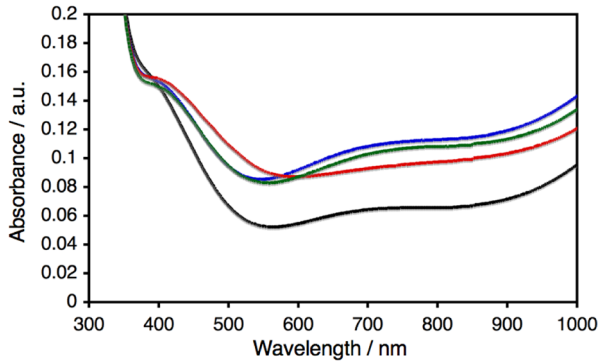

Figure 4. UV/vis absorption spectrum ITO and EDOT-based polymer films. ITO modified with SAM of terthiophene (black) and 25 nm thick polyelectrolyte film with 35% EDOT−SuNa content doped in Millipore water (blue) and doped in aqueous $LiClO_4$ solution (green). The absorption of the same film reduced in aqueous $LiClO_4$ solution is shown in red.

difficult to compare FF and J_{SC} against the PEDOT:PSS standard device and compared only the V_{OC} and R_S data with those for PEDOT:PSS and previously reported ePEDOT films (a more detailed description of the substrate architecture and its influence on the active layer can be found in the Supporting Information, Figure S8).

The PEDOT:PSS films were annealed at 120 °C for 10 min to remove residual water, which influences the film work function leading to the commonly observed work function values of up to 5.2 eV.[84] All polyelectrolyte films were found to release water very easily in vacuum, which is why we did not perform annealing for these buffer layers.

As expected, the work function of the film-covered ITO showed a large impact on the V_{OC} of the OPV device. For instance, the V_{OC} increased depending on the buffer layer work function from 0.30 V for pure ePEDOT in entry 1 to 0.60 V for the polyelectrolyte EDOT/EDOT−SuNa copolymer film in entry 4 as seen in Figure 5.

Table 1. OPV Bulk Heterojunction Device Data Using P3HT:PCBM in the Active Layer with Different Anode Buffers[a]

entry	anode buffer	EDOT−SuNa content (%)	work function (eV)	V_{OC} (V)	R_S (Ω cm^2)	PCE (%)
1	ePEDOT (perchlorate-doped)	0	4.8	0.30	2.3	0.18
2	polyelectrolyte (self-doped)	35	4.9	0.35	4.0	1.1
3	polyelectrolyte (self-doped)	50	5.0	0.45	2.3	0.33
4	polyelectrolyte (perchlorate-doped)	50	5.2	0.60	4.0	0.99
5	PEDOT:PSS		5.1−5.2	0.57	2.5	2.6
6	ePEDOT (doped with $LiClO_4$, ref 31)	0	not reported	0.48	–	1.1
7	ePEDOT (doped with NaPSS, ref 28)	0	4.87 eV	0.43	–	1.51

[a]The last two entries are taken from refs 31 and 28, respectively, which we used here to compare our devices with previously reported ones.

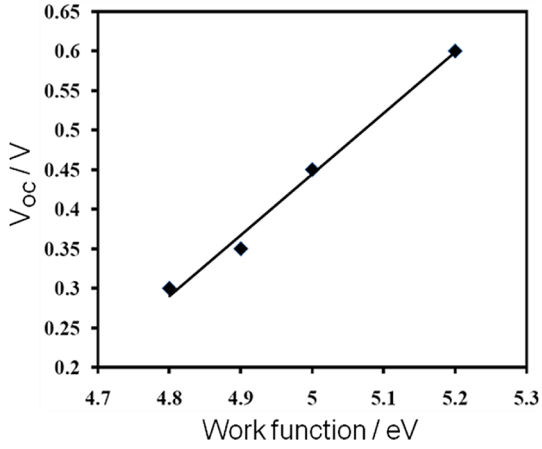

Figure 5. Relationship of work function of ePEDOT buffer layer and V_{OC} values of OPV device data (entries 1−4 of Table 1).

The V_{OC} of the ePEDOT film with the highest work function was similar to that of PEDOT:PSS buffer and higher than those previously reported for ePEDOT films (entries 6 and 7), which suggests a lower work function for these films.

The low overall R_S values indicate that all ePEDOT buffer layers are highly conductive. The low efficiency values are because of the lower FF and J_{SC} of these devices that arise from the above-mentioned difference of the device architecture (see Supporting Information for J_{SC} and FF data). The incident photon-to-current conversion efficiency (IPCE) data (Figure 6) are lower for the devices built with our buffer for the whole absorption range indicating the lower J_{SC} currents are not because of higher buffer resistance but due to other reasons such as less efficient exciton dissociation in the active layer. Note that the devices with PEDOT:PSS (solid blue line in Figure 6) and polyelectrolyte buffer of entry 2 (solid red line)

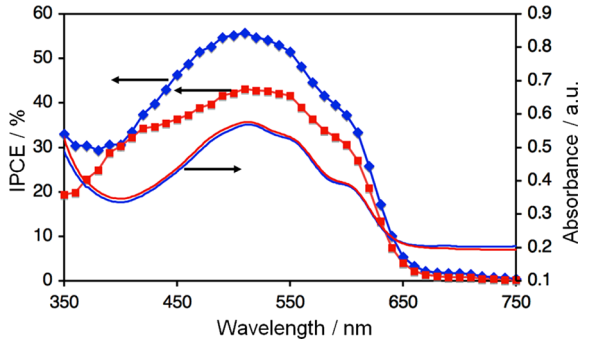

Figure 6. IPCE values of OPV devices. Blue diamonds are used for the PEDOT:PSS anode buffer layer and red squares for the self-doped polyelectrolyte (35% EDOT−SuNa, entry 2 in Table 1). The UV/vis absorption spectra of films of the structure ITO/PEDOT/P3HT:PCBM are shown as a solid red line for the electropolymerized and self-doped polyelectrolyte and a solid blue line for PEDOT:PSS.

have the same absorption, indicating similar oxidized and transparent buffer films (non-normalized spectra in Supporting Information, Figure S9).

Although the work function and V_{OC} indicate a clear mutual dependency, the behavior of the FF and J_{SC} do not show any trend, because of the above-mentioned difference of device structure. We envision further enhancing the device efficiencies by surface energy optimization and the use of other types of substrates. It is indeed known that the surface energy of the bottom electrode strongly affects the morphology of the active layer, leading to better morphologies with films of enhanced hydrophobicity, for example, by inducing a vertical phase separation of the two components in the active layer[85−88] or influencing the P3HT and PCBM aggregation size,[36,89,90] which affects the J_{SC} value by losses in photocurrent[91] and efficiency in charge separation,[36] respectively.

The tuning of film work function and hydrophobicity using anionic polyelectrolytes observed here opens up a fascinating way for the design of new optimized anode interlayers for interface optimization and will be the subject of future studies using different organic semiconductors and device architectures, such as *p*−*i*−*n* heterojunctions.[92]

CONCLUSION

We reported new conductive polyelectrolyte films with tunable work function and hydrophobicity for a specifically optimized anode buffer layer in organic electronic devices. We successfully linked these film properties to the functional groups attached on the ePEDOT side chain and the EDOT copolymer composition. The copolymers introduced here can overcome the mutually exclusive conductivity−high work function relationship of previously conductive buffer layers by reaching high work functions without the need for any insulating or acidic additives. We demonstrated a clear influence of the film work function on OPV device performance, proving the importance of such a tunable buffer layer in organic electronic devices. The results here will allow the rational design of new anode buffers specifically optimized for the organic semiconductors used in the active layer of the device. In addition, the facile production technique from aqueous solution using easily accessible EDOT monomers will be beneficial for applications in industrial production techniques. Finally, we confirmed the utility of the PYS instrument for determination of work function values, as was recently reported.[59]

ASSOCIATED CONTENT

Supporting Information

Detailed information about the synthetic, SAM-building film polymerization and OPV device building procedures and all remaining data such as buffer AFM images. This material is available free of charge via the Internet at http://pubs.acs.org.

AUTHOR INFORMATION

Corresponding Author

*E-mail: matsuo@chem.s.u-tokyo.ac.jp (Y.M.), nakamura@chem.s.u-tokyo.ac.jp (E.N.).

Notes

The authors declare no competing financial interest.

ACKNOWLEDGMENTS

This work was supported by the Strategic Promotion of Innovative Research and Development from the Japan Science and Technology Agency, JST and KAKENHI (22000008 for E.N.), 21750136 and by the Funding Program for Next-Generation World-Leading Researchers (to Y.M.). S.L. thanks the Global COE program (MEXT) for financial support. H.-h.Y. and S.-C.L. thank RIKEN Advanced Science Institute and Grant-in-Aid for Young Scientists (No. 22681016 and 23700565), JSPS/MEXT, Japan, for financial support. B.Z. thanks RIKEN for a Special Postdoctoral Researcher Fellowship.

REFERENCES

(1) Service, R. F. *Science* **2011**, *332*, 293.
(2) Green, M. A.; Emery, K.; Hishikawa, Y.; Warta, W.; Dunlop, E. D. *Prog. Photovoltaics* **2012**, *20*, 12−20.
(3) Sirringhaus, H.; Tessler, N.; Friend, R. H. *Science* **1998**, *280*, 1741−1744.
(4) Aziz, H.; Popovic, Z. D.; Hu, N. X.; Hor, A. M.; Xu, G. *Science* **1999**, *283*, 1900−1902.
(5) Ravirajan, P.; Peiro, A. M.; Nazeeruddin, M. K.; Graetzel, M.; Bradley, D. D. C.; Durrant, J. R.; Nelson, J. *J. Phys. Chem. B* **2006**, *110*, 7635−7639.
(6) Goh, C.; Scully, S. R.; McGehee, M. D. *J. Appl. Phys.* **2007**, *101*, 114503.
(7) Hwang, E.; Nalin de Silva, K. M.; Seevers, C. B.; Li, J.-R.; Garno, J. C.; Nesterov, E. E. *Langmuir* **2008**, *24*, 9700−9706.
(8) Di, C.-A.; Liu, Y.; Yu, G.; Zhu, D. *Acc. Chem. Res.* **2009**, *42*, 1573−1583.
(9) Brown, T. M.; Kim, J. S.; Friend, R. H.; Cacialli, F.; Daik, R.; Feast, W. J. *Synth. Met.* **2000**, *111*, 285−287.
(10) Campbell, A. J.; Bradley, D. D. C.; Antoniadis, H. *Synth. Met.* **2001**, *122*, 161−163.
(11) Irwin, M. D.; Buchholz, D. B.; Hains, A. W.; Chang, R. P. H.; Marks, T. J. *Proc. Natl. Acad. Sci. U.S.A.* **2008**, *105*, 2783−2787.
(12) Nakayama, Y.; Moorii, K.; Suzuki, Y.; Machida, H.; Krea, S.; Ueno, N.; Kitagawa, H.; Noguchi, Y.; Ishii, H. *Adv. Funct. Mater.* **2009**, *19*, 3746−3752.
(13) Hains, A. W.; Liu, J.; Martinson, A. B. F.; Irwin, M. D.; Marks, T. J. *Adv. Funct. Mater.* **2010**, *20*, 595−606.
(14) Ecker, B.; Nolasco, J. C.; Pallarés, J.; Marsal, L. F.; Posdorfer, J.; Parisi, J.; von Hauff, E. *Adv. Funct. Mater.* **2011**, *21*, 2705−2711.
(15) de Jong, M. P.; van Ijzendoorn, L. J.; Voigt, M. J. A. *Appl. Phys. Lett.* **2000**, *77*, 2255−2257.
(16) Nguyen, T. P.; de Vos, S. A. *Appl. Surf. Sci.* **2004**, *221*, 330−339.
(17) Sharma, A.; Andersson, G.; Lewis, D. A. *Phys. Chem. Chem. Phys.* **2011**, *13*, 4381−4387.
(18) Lee, H. J.; Lee, J.; Park, S.-M. *J. Phys. Chem. B* **2010**, *114*, 2660−2666.

(19) Pingree, L. S. C.; MacLeod, B. A.; Ginger, D. S. *J. Phys. Chem. C* **2008**, *112*, 7922−7927.
(20) Armstrong, N. R.; Veneman, P. A.; Ratcliff, E.; Placencia, D.; Brumbach, M. *Acc. Chem. Res.* **2009**, *42*, 1748−1757.
(21) Koch, N. *ChemPhysChem* **2007**, *8*, 1438−1455.
(22) Lee, T.-W.; Chung, Y. *Adv. Funct. Mater.* **2008**, *18*, 2246−2252.
(23) Koch, N.; Vollmer, A. *Appl. Phys. Lett.* **2006**, *89*, 162107.
(24) Tengstedt, C.; Osikowicz, W.; Salaneck, W. R.; Parker, I. D.; Hsu, C. H.; Fahlman, M. *Appl. Phys. Lett.* **2006**, *88*, 053502.
(25) Choi, M.-R.; Han, T.-H.; Lim, K.-G.; Woo, S.-H.; Huh, D. H.; Lee, T.-W. *Angew. Chem., Int. Ed.* **2011**, *50*, 6274−6277.
(26) Gu, C.; Liu, H.; Hu, D.; Zhang, W.; Lv, Y.; Lu, P.; Lu, D.; Ma, Y. *Macromol. Rapid Commun.* **2011**, *32*, 1014−1019.
(27) Zotti, G.; Zecchin, S.; Schiavon, G.; Louwet, F.; Groenendaal, L.; Crispin, X.; Osikowicz, W.; Salaneck, W.; Fahlman, M. *Macromolecules* **2003**, *36*, 3337−3344.
(28) Rider, D. A.; Harris, K. D.; Wang, D.; Bruce, J.; Fleischauer, M. D.; Tucker, R. T.; Brett, M. J.; Buriak, J. M. *ACS Appl. Mater. Interfaces* **2009**, *1*, 279−288.
(29) Armstrong, N. R.; Carter, C.; Donley, C.; Simmonds, A.; Lee, P.; Brumbach, M.; Kippelen, B.; Domercq, B.; Yoo, S. *Thin Solid Films* **2003**, *445*, 342−353.
(30) Yan, J.; Sun, C.; Tan, F.; Hu, X.; Chen, P.; Qu, S.; Zhou, S.; Xu, J. *Sol. Energy Mater. Sol. Cells* **2010**, *94*, 390−394.
(31) Nasybulin, E.; Wei, W.; Cox, M.; Kymissis, I.; Levon, K. *J. Phys. Chem. C* **2011**, *115*, 4307−4314.
(32) Huang, J.-H.; Ho, Z.-Y.; Kekuda, D.; Chu, C.-W.; Ho, K.-C. *J. Phys. Chem. C* **2008**, *112*, 19125−19130.
(33) Mauger, S. A.; Moulé, A. J. *Org. Electron.* **2011**, *12*, 1948−1956.
(34) Kim, Y. H.; Sachse, C.; Machala, M. L.; May, C.; Müller-Meskamp, L.; Leo, K. *Adv. Funct. Mater.* **2011**, *21*, 1076−1081.
(35) Mihailetchi, V. D.; Blom, P. W. M.; Hummelen, J. C.; Rispens, M. T. *J. Appl. Phys.* **2003**, *94*, 6849−6854.
(36) Bulliard, X.; Ihn, S.-G.; Yun, S.; Kim, Y.; Choi, D.; Choi, J.-Y.; Kim, M.; Sim, M.; Park, J.-H.; Choi, W.; Cho, K. *Adv. Funct. Mater.* **2010**, *20*, 4381−4387.
(37) Cheyns, D.; Poortmans, J.; Heremans, P.; Deibel, C.; Verlaak, S.; Rand, B. P.; Genou, J. *Phys. Rev. B* **2008**, *77*, 165332.
(38) Brabec, C.; Cravino, A.; Meissner, D.; Sariciftci, N.; Fromherz, T.; Rispens, M.; Sanches, L.; Hummel, J. *Adv. Funct. Mater.* **2001**, *11*, 374−380.
(39) Tress, W.; Leo, K.; Riede, M. *Adv. Funct. Mater.* **2011**, *21*, 2140−2149.
(40) Dietrich, M.; Heinze, J.; Heywang, G.; Jonas, F. *J. Electroanal. Chem.* **1994**, *369*, 87−92.
(41) Yamato, H.; Ohwa, M.; Wernet, W. *J. Electroanal. Chem.* **1995**, *397*, 163−170.
(42) Jonas, F.; Louwet, F.; Cloots, T.; Groenendaal, L. Process for the Preparation of Water-Soluble pi-Conjugated Polymers. U.S. Patent 6,635,729, October 21, 2003.
(43) Stéphan, O.; Schottland, P.; Le Gall, P.-Y.; Chevrot, C.; Mariet, C.; Carrier, M. *J. Electroanal. Chem.* **1998**, *443*, 217−226.
(44) Koch, N.; Elschner, A.; Rabe, J. P.; Johnson, R. L. *Adv. Mater.* **2005**, *17*, 330−335.
(45) Kang, J. F.; Perry, J. D.; Tian, P.; Kilbey, S. M., II. *Langmuir* **2002**, *18*, 10196−10201.
(46) Hwang, E.; Nalin de Silva, K. M.; Seevers, C. B.; Li, J.-R.; Garno, J. C.; Nesterov, E. E. *Langmuir* **2008**, *24*, 9700−9706.
(47) Armstrong, N. R.; Carter, C.; Donley, C.; Simmonds, A.; Lee, P.; Brumbach, M.; Kippelen, B.; Domercq, B.; Yoo, S. *Thin Solid Films* **2003**, *445*, 342−352.
(48) Xia, C.; Advincula, R. C. *Chem. Mater.* **2001**, *13*, 1682−1691.
(49) Spanninga, S. A.; Martin, D. C.; Chen, Z. *J. Phys. Chem. C* **2010**, *114*, 14992−14997.
(50) Kayinamura, Y. P.; Ovadia, M.; Zavitz, D.; Rubinson, J. F. *ACS Appl. Mater. Interfaces* **2010**, *2*, 2653−2662.
(51) Han, D.-H.; Kim, J.-W.; Park, S.-M. *J. Phys. Chem. B* **2006**, *110*, 14874−14880.
(52) Sakmeche, N.; Aeiyach, S.; Aaron, J.-J.; Jouini, M.; Lacroix, J. C.; Lacaze, P.-C. *Langmuir* **1999**, *15*, 2566−2574.
(53) Luo, S.-C.; Mohamed Ali, E.; Tansil, N. C.; Yu, H.-h.; Gao, S.; Kantchev, E. A. B.; Ying, J. Y. *Langmuir* **2008**, *24*, 8071−8077.
(54) Cho, S. H.; Lee, H. J.; Ko, Y.; Park, S.-H. *J. Phys. Chem. C* **2011**, *113*, 6545−6553.
(55) Poverenov, E.; Li, M.; Bitler, A.; Bendikov, M. *Chem. Mater.* **2010**, *22*, 4019−4025.
(56) Doherty, W. J., III; Wysocki, R. J.; Armstrong, N. R.; Saavedra, S. S. *Macromolecules* **2006**, *39*, 4418−4424.
(57) Otero, T. F.; Grande, H.; Rodríges, J. *J. Electroanal. Chem* **1995**, *394*, 211−216.
(58) Randriamahazaka, H. *Smart Mater. Struct.* **2011**, *20*, 124010.
(59) Lacher, S.; Matsuo, Y.; Nakamura, E. *J. Am. Chem. Soc.* **2011**, *113*, 16997−17004.
(60) Ratcliff, E. L.; Lee, P. A.; Armstrong, N. R. *J. Mater. Chem.* **2010**, *20*, 2672−2679.
(61) Seo, J. H.; Nguyen, T.-Q. *J. Am. Chem. Soc.* **2008**, *130*, 10042−10043.
(62) Hoven, C. V.; Yang, R.; Garcia, A.; Crockett, V.; Heeger, A. J.; Bazan, G. C.; Nguyen, T.-Q. *Proc. Natl. Acad. Sci. U.S.A.* **2008**, *105*, 12730−12735.
(63) Bolink, H. J.; Brine, H.; Coronado, E.; Sessolo, M. *ACS Appl. Mater. Interfaces* **2010**, *2*, 2694−2698.
(64) Seo, J. H.; Gutacker, A.; Walker, B.; Cho, S.; Garcia, A.; Yang, R.; Nguyen, T.-Q.; Heeger, A. J.; Bazan, G. C. *J. Am. Chem. Soc.* **2009**, *131*, 18220−18221.
(65) Seo, J. H.; Namdas, E. B.; Gutacker, A.; Heeger, A. J.; Bazan, G. C. *Appl. Phys. Lett.* **2010**, *97*, 043303.
(66) Luo, J.; Wu, H.; He, C.; Li, A.; Yang, W.; Cao, Y. *Appl. Phys. Lett.* **2009**, *95*, 043301.
(67) He, C.; Zhong, C.; Wu, H.; Yang, R.; Yang, W.; Huang, F.; Bazan, G. C.; Cao, Y. *J. Mater. Chem.* **2010**, *20*, 2617−2622.
(68) Oh, S.-H.; Na, S.-I.; Jo, J.; Lim, B.; Vak, D.; Kim, D.-Y. *Adv. Funct. Mater.* **2010**, *20*, 1977−1983.
(69) Seo, J. H.; Gutacker, A.; Sun, Y.; Wu, H.; Huang, F.; Cao, Y.; Scherf, U.; Heeger, A. J.; Bazan, G. C. *J. Am. Chem. Soc.* **2001**, *133*, 8414−8419.
(70) Wu, H.; Huang, F.; Mo, Y.; Yang, W.; Wang, D.; Peng, J.; Cao, Y. *Adv. Mater.* **2004**, *16*, 1826−1830.
(71) Gross, M.; Müller, D. C.; Nothofer, H.-G.; Scherf, U.; Neher, D.; Bräuchle, C.; Meerholz, K. *Nature* **2000**, *405*, 661−665.
(72) Frohne, H.; Müller, D. C.; Merrholz, K. *ChemPhysChem* **2002**, *3*, 707−711.
(73) Frohne, H.; Shaheen, S. E.; Brabec, C. J.; Müller, D. C.; Sariciftci, N. S.; Meerholz, K. *ChemPhysChem* **2002**, *3*, 795−799.
(74) Petr, A.; Zhang, F.; Peisert, H.; Knupfer, M.; Dunsch, L. *Chem. Phys. Lett.* **2004**, *385*, 140−143.
(75) Zhang, F.; Petr, A.; Dunsch, L. *Appl. Phys. Lett.* **2003**, *82*, 4587−4589.
(76) Zhang, F.; Petr, A.; Peisert, H.; Knupfer, M.; Dunsch, L. *J. Phys. Chem. B* **2004**, *108*, 17301−17305.
(77) Wuyang, J.; Xu, Q.; Chu, C.-W.; Yang, Y.; Li, G.; Shinar, J. *Polymer* **2004**, *45*, 8443−8450.
(78) Tada, A.; Geng, Y.; Wei, Q.; Hashimoto, K.; Tajima, K. *Nat. Mater.* **2011**, *10*, 450−455.
(79) Luo, S.-C.; Liour, S. S.; Yu, H.-h. *Chem. Commun.* **2010**, *46*, 4731−4733.
(80) Schwendeman, I.; Graupp, C. L.; Hancock, J. M.; Groenendaal, B.; Reynolds, J. R. *Adv. Funct. Mater.* **2003**, *13*, 541−547.
(81) Tansil, N. C.; Kantchev, E. A. B.; Gao, Z.; Yu, H.-h. *Chem. Commun.* **2011**, *47*, 1533−1535.
(82) Xie, H.; Luo, S.-C.; Yu, H.-h. *Small* **2011**, *5*, 2611−2617.
(83) Luo, S.-C.; Xie, H.; Chen, N.; Yu, H.-h. *ACS Appl. Mater. Interfaces* **2009**, *1*, 1414−1419.
(84) Koch, N.; Vollmer, A.; Elschner, A. *Appl. Phys. Lett.* **2007**, *90*, 043512.

(85) Arias, A. C.; Corcoran, N.; Banach, M.; Friend, R. H.; MacKenzie, J. D.; Huck, W. T. S. *Appl. Phys. Lett.* **2002**, *80*, 1695−1698.
(86) Björström, C. M.; Nilsson, S.; Bernasik, A.; Budkowski, A.; Andersson, M.; Magnusson, K. O.; Moons, E. *Appl. Surf. Sci.* **2007**, *253*, 3906−3912.
(87) Campoy-Quiles, M.; Ferenczi, T.; Agostinelli, T.; Etchegoin, P. G.; Kim, Y.; Anthopoulos, T. D.; Stavrinou, P. N.; Bradley, D. C.; Nelson, J. *Nat. Mater.* **2008**, *7*, 158−164.
(88) Chen, L.-M.; Hong, Z.; Li, G.; Yang, Y. *Adv. Mater.* **2009**, *21*, 1434−1449.
(89) Wei, J. H.; Coffey, D. C.; Ginger, D. S. *J. Phys. Chem. B* **2006**, *110*, 24324−24330.
(90) Park, L. Y.; Munro, A. M.; Ginger, D. S. *J. Am. Chem. Soc.* **2008**, *130*, 15916−15926.
(91) Lyons, B. P.; Clarke, N.; Groves, C. *J. Phys. Chem. C* **2011**, *115*, 22572−22577.
(92) Matsuo, Y.; Sato, Y.; Niinomi, T.; Soga, I.; Tanaka, H.; Nakamura, E. *J. Am. Chem. Soc.* **2009**, *131*, 16048−16050.